

Soldering of Mg Joints Using Zn-Al Solders



TOMASZ GANCARZ, KATARZYNA BERENT, WOJCIECH SKUZA,
and KATARZYNA JANIK

Magnesium has applications in the automotive and aerospace industries that can significantly contribute to greater fuel economy and environmental conservation. The Mg alloys used in the automotive industry could reduce mass by up to 70 pct, providing energy savings. However, alongside the advantages there are limitations and technological barriers to use Mg alloys. One of the advantages concerns phenomena occurring at the interface when joining materials investigated in this study, in regard to the effect of temperature and soldering time for pure Mg joints. Eutectic Zn-Al and Zn-Al alloys with 0.05 (wt pct) Li and 0.2 (wt pct) Na were used in the soldering process. The process was performed for 3, 5, and 8 minutes of contact, at temperatures of 425 °C, 450 °C, 475 °C, and 500 °C. Selected, solidified solder-substrate couples were cross-sectioned, and their interfacial microstructures were investigated by scanning electron microscopy. The experiment was designed to demonstrate the effect of time, temperature, and the addition of Li and Na on the kinetics of the dissolving Mg substrate. The addition of Li and Na to eutectic Zn-Al caused to improve mechanical properties. Higher temperatures led to reduced joint strength, which is caused by increased interfacial reaction.

<https://doi.org/10.1007/s11661-018-4617-0>
© The Author(s) 2018

I. INTRODUCTION

CHANGES to the electrical engine, which can bring about a reduction in its mass, are of significant interest to the automotive industry.^[1,2] Al and Mg alloys are increasingly used to reduce structural mass.^[3] Taking into account the lightest applications, the density of structural materials ($\rho_{Al} = 2.7 \text{ g cm}^{-3}$, $\rho_{Mg} = 1.7 \text{ g cm}^{-3}$)^[4] is very important. The aerospace industry's requirements for lightweight materials to operate under increasingly demanding conditions calls for reduced mass and improved mechanical properties. Compared to the Al alloys, the Mg alloys display better physical and mechanical properties, such as high strength-to-weight ratio, high damping capacity, and a high recycling potential. These facts could have a decisive effect on the application of Mg alloys in the automotive, electronics, and aerospace industries. However, similar atomic mass and melting temperature in the Al-Mg system formed brittle intermetallic compounds (IMCs) such as Al_3Mg_2 and $Al_{12}Mg_{17}$ in the solidified metal.^[5] Furthermore, joining the Al with Mg alloys is difficult, but possible using several

techniques such as resistant spot welding,^[3,6] reactive brazing,^[7] laser welding,^[8] ultrasonic-assisted soldering,^[9] and so on. In order to eliminate the negative effect of Mg-Al IMCs on the strength of the joints, an interlayer intended to block the formation of brittle IMC^[3] was used. Zn,^[3] Sn-Zn alloys,^[10] Mg-Zn-Al, and Mg-In-Zn^[11] were used to join Al with Mg alloys.

In view of the high oxidation and corrosion of Mg alloys, an addition characterized by high electrode potential compared to Mg (-2.37 V)^[9] is made to the solder. In this case, the layers of chromium and Teflon protected the Mg against corrosion.^[12] Mg alloys soldered at high temperature displayed worse mechanical properties, so the joining process temperature should be lower than 450 °C. For lower temperature soldering, flux was used to increase wettability, which also protected the alloy surface from the formation the stable magnesium oxide.^[11] The application of an Zn interlayer when joining Al/Mg alloys using resistant spot welding caused a reduction in welding current compared with traditional welding.^[3] Al dissolving into the fusion zone caused the increased formation of solid particles, which improves the quality of the joints.^[3] Sn-Zn used at low temperatures for soldering Al/Mg joints caused the amount of Zn to rise by up to 30 pct, increasing shear strength. In addition, the dispersive distribution of the Al-Sn-Zn solid solution within the solder reduced the brittleness of the joint, thus greatly improving the mechanical properties. The conducted study, joining AZ31B alloy using Zn, caused the formation of an IMC from the Zn-Mg system at the interface. However, a higher cooling rate

TOMASZ GANCARZ, WOJCIECH SKUZA, and KATARZYNA JANIK are with the Institute of Metallurgy and Materials Science, Polish Academy of Sciences, 30-059 Krakow, Poland. Contact e-mail: t.gancarz@imim.pl KATARZYNA BERENT is with the AGH University of Science and Technology, Academic Centre for Materials and Nanotechnology, 30-059 Krakow, Poland.

Manuscript submitted May 24, 2017.

Article published online April 18, 2018

was beneficial for increasing the tensile shear strength of joints,^[9] as it caused the formation of equiaxed dendrites and refined eutectic structure.

To show the influence at the interface during soldering, research should be carried out for pure Mg. This study demonstrates the effect on the microstructure of joints and mechanical properties of joining pure Mg using eutectic Zn-Al and Zn-Al alloys with additions of Li and Na.

II. EXPERIMENTAL

Cast alloys of eutectic Zn-Al,^[13] Zn-Al0.05Li,^[13] and Zn-Al0.2Na^[14] were used in this study, and the solder was tested while soldering Cu substrate.^[15,16] The cast alloys were rolled to a thickness of 1 mm and cut into 8 × 10 mm pieces. The base material used for soldering was pure Mg (99.9 pct) with dimensions of 8 × 4 × 25 mm. The Mg substrate and solder pieces were cleaned using emery paper and acetone before the soldering process, to remove the oxide from the surface. Soldering the Mg joints was carried out using the sessile drop method,^[17] with protective gas Ar (5N), for times of 3, 5, and 8 minutes of contact and at temperatures of 425 °C, 450 °C, 475 °C, and 500 °C. The samples were moved from the cold zone to the hot zone of the furnace, where a type K thermocouple was touching the bottom of the holder and the melting process was observed by CCD camera. After a predetermined time, the sample was moved to the cold zone, then removed and placed on a stone table. A special holder (the same as was used in Reference 18) was employed during the process, to keep together the Mg substrate. After the soldering process, the overflow of solder was gently removed in order to preserve the dimensions of the samples. Four samples were prepared for each temperature and time, three for testing of mechanical properties and one for microstructure observation. The specimens for cross section were mounted in resin, than grand and polished. Microstructural and elemental analyses were performed using scanning electron microscopy (FEI Quanta 3D FEG-SEM) coupled with energy dispersive X-ray spectrometry (EDS), in order to study the interfacial

microstructure and IMCs occurring at the interface. For all samples, three measurements were made at different areas to improve statistics and to check the homogeneity of the joints. Mechanical tests were conducted with an INSTRON 6025 testing machine modernized by Zwick/Roell. Testing conditions were in accordance with ASTM A 264-03, with a strain rate of 0.00025 (1/s) at room temperature. The mechanical tests were performed for each of the joints with the eutectic Zn-Al alloys, and with Na and Li additions, and three successful measurements were taken. After mechanical testing, the real area of the joints (the area of soldering between Mg substrates) was measured using CorelDraw with the GetArea module. The shear strength is calculated using the obtained force from mechanical tests divided by real area of the joints. The samples for the tests were taken after soldering, where the flow solder from the substrate was removed. The microhardness of the formed phases in the soldering region was measured by means of microhardness tests carried out at a load of 0.5 (N) and over a time of 15 (seconds).

III. RESULTS

A. Microstructure Observation

All the Mg joints were obtained under a suitable protective gas without flux. However, an experiment using flux and without protective gas was also performed. Fluxes such as ALU12, QJ201, F380Mg, and F390Mg caused the joints' mechanical properties to worsen, and even led to the joints themselves breaking. Taking this into account, a protective atmosphere was used instead of flux, and this resulted in stable joints. The microstructure is presented in Figure 1, for eutectic Zn-Al and Mg joints after soldering for 3, 5, and 8 minutes of contact, at a temperature of 425 °C. The solder dissolved Mg substrates during the soldering process, and formed at the interface an interfacial Mg-Zn layer, which was confirmed by the EDS analysis presented in Table I. With increasing soldering time, the Mg-Zn layer grew. Furthermore, particles of Mg with a small amount of Zn dissolved inside the filler solder.

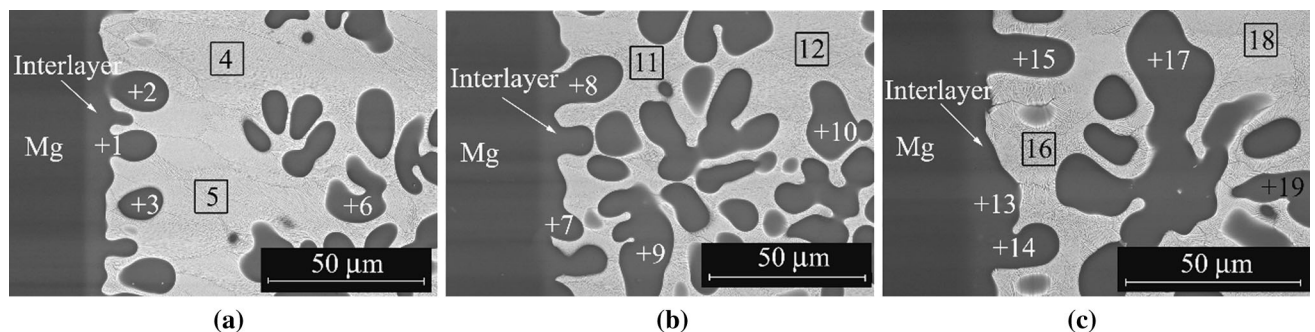


Fig. 1—Microstructure after soldering process for eutectic Zn-Al and Mg joints for (a) 3, (b) 5, and (c) 8 min of contact, at a temperature of 425 °C. The numbers in the figure denote the points of EDSs presented in Table I.

The amount of Al is on the same level for all measured points, at around 2 to 3 (wt pct). However, the Zn in the Mg-Zn particles increased slightly from the Mg substrate (~ 3 wt pct) to inside the solder (~ 8 wt pct), which correlates with Mg dissolving in the solder. The Mg particles in all soldered joints were observed. Most importantly, the matrix of the solder changed from eutectic Zn-Al to an Mg + MgZn eutectoid structure. This reaction is correlated with the high amount of dissolved Mg, which, according to the Mg-Zn phase diagram,^[5] formed the lamellar α - Mg + MgZn eutectoid structure distributed on the boundary of the black α -Mg solid solution in the soldering region. EDS analysis (Table I—gray area) shows that, with increasing time, the amount of Mg in these eutectoid areas also increases. According to the Mg-Zn phase diagram,^[5] the Mg₇Zn₃ phase is formed by a eutectic reaction at 340 °C: $L \rightarrow \alpha - Mg + Mg_7Zn_3$. Further reduction of temperature causes the formation

of an MgZn phase by a eutectoid reaction at 325 °C: $Mg_7Zn_3 \rightarrow \alpha - Mg + MgZn$.^[19] However, in our case, Mg was dissolving and supplied to the melt solder, which is observed in the microstructure (Figure 1). With increasing time, a rising number of Mg particles is observed, with the highest being for 8 min. A similar microstructure for all eutectic Zn-Al and Zn-Al with Li and Na alloys was observed. However, under the same conditions, the highest amount of dissolved Mg in the interface, and the greatest number of Mg particles for Na content, was observed for Zn-Al0.05Li compared to eutectic Zn-Al (see Figure 2). In Figure 2, (a) Zn-Al, (b) Zn-Al0.05Li, and (c) Zn-Al0.2Na joints after soldering at 450 °C and 8 minutes are presented.

Figure 3 shows the Mg joints soldered by eutectic Zn-Al after 3 minutes and at temperatures of 450 °C, 475 °C, and 500 °C. With increasing temperature, the Al-Mg interlayers obtained greater thickness and a higher number of Mg inclusions are observed.

According to the Mg-Li^[20] phase diagrams, Li content up to 5 (wt pct) dissolved in the solid solution. For Na content (in the whole range) as shown in Mg-Na,^[21] the liquid occurring across almost the entire Mg range of Mg-Na alloys after 97.8 °C probably accelerates the dissolving process of Mg substrates. The greatest dissolution with soldering time for Li and Na-containing alloys compared to eutectic Zn-Al is presented in Figure 4.

The measured thickness of the “interlayer” is dependent on the time. With increasing temperature and time, the thickness of the interlayer also increased. This effect caused the Mg substrate to dissolve by the grain boundary, and all grains to move to the solder, which is shown for Na content in eutectic Zn-Al in Figure 2(c). The data presented in Figure 4 confirm that, with time and temperature of soldering, the effect of dissolving Mg substrates is highest for Na, then for Li additions, and lowest for eutectic Zn-Al.

The microstructure for 425 °C is presented in Figure 1(a). With increasing temperature, the amount of dissolved Mg in the solder also increases. At the highest temperature (500 °C), dissolution of the Mg substrate by the grain boundary is observed after 3 minutes, to the same degree as after 8 minutes at a lower temperature, of 450 °C. For all alloys, eutectic Zn-Al, and Zn-Al with Li and Na additions, the

Table I. EDS Analysis of Marked Points in Fig. 1 of Soldering Joints with Increasing Time of 3, 5, and 8 Min at a Temperature of 425 °C

	Weight Percent		
	MgK	AlK	ZnK
1	91.1	2.1	6.8
2	90.5	2.1	7.4
3	90.8	2.1	7.1
4	49.4	3.2	47.4
5	49.5	3.0	47.5
6	90.0	2.0	8.0
7	91.3	2.1	6.6
8	90.9	2.4	6.7
9	90.9	2.2	6.9
10	90.5	2.2	7.3
11	50.2	3.4	46.4
12	50.1	3.6	46.3
13	91.3	2.3	6.4
14	92.0	2.3	5.7
15	90.4	2.4	7.2
16	54.0	3.6	42.4
17	91.2	2.4	6.4
18	51.6	3.8	44.6
19	90.5	2.5	7.0

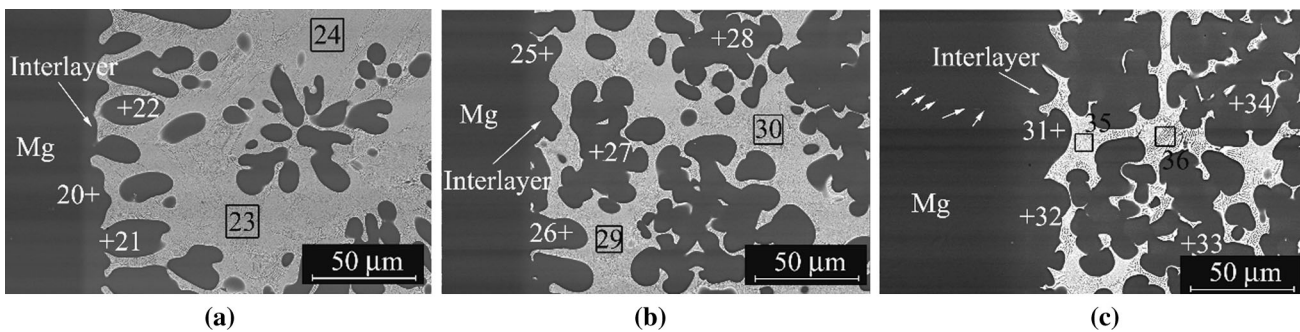


Fig. 2—Microstructure after soldering process for (a) Zn-Al, (b) Zn-Al0.05Li, (c) Zn-Al0.2Na, respectively, at 450 °C for 8 min. The numbers in the figure denote the points of EDSs presented in Table II.

observed microstructures are similar. However, the thickness of the interlayer at the interface increases with additions of Li and Na compared to eutectic Zn-Al, as shown in Figure 4. For the highest soldering temperature, of 500 °C, the dissolution of all Mg grains is observed for all alloys, which caused increasing consumption of the Mg substrate, an increase in the thickness of the interlayer, and a resulting increase in the thickness of the area of the joints.

B. Mechanical Properties

At first, tensile tests were used to determine the shear strength of joints.^[9,10,19] However, during our tensile testing the sample was twisted, causing the Mg substrate to break close to the soldering zone, which increased the errors in calculating the shear strength of the joints. As a result, a different method of tensile testing was proposed in order to obtain the correct shear strength of joints. As described in Reference 22, the soldered pad is sheared

during applied force. Such a solution ensuring the correct shear strength of joints was applied.

To determine the shear strength of joints, the device presented in Reference 22 and Figure 5 was used, along with samples of different diameters. However, especially for the high temperature of 500 °C, the Mg pads are dissolved by the solder during the soldering process, causing the area of interface reaction to move and expand. The obtained results for the shear strengths of joints with eutectic Zn-Al, Zn-Al0.05Li, and Zn-Al0.2Na, after soldering times of 3, 5, and 8 minutes and for temperatures of 425 °C, 450 °C, 475 °C, and 500 °C are presented in Figure 6.

Zn-Al0.2Na showed the highest shear strength value (50.7 MPa), followed by Zn-Al0.05Li (32.2 MPa) and eutectic Zn-Al (28.2 MPa). For all solders, the highest values of shear strength of joints for temperatures of 425 °C, 450 °C, and 475 °C were obtained for all times. These values are all similar and fall within error limits. For a soldering temperature of 500 °C, shear strength reduces significantly, by as much as 50 pct, in all cases. Such behavior could be caused by the increasing

Table II. EDS Analysis of Marked Points in Fig. 2 of Soldering Mg Joints at a Temperature of 450 °C and a Time of 8 Min, by Eutectic Zn-Al, Zn-Al0.05Li, and Zn-Al0.2Na

	Weight Percent		
	MgK	AlK	ZnK
20	91.5	1.9	6.6
21	90.9	1.9	7.2
22	90.4	1.9	7.7
23	49.7	3.0	47.3
24	49.4	3.0	47.6
25	92.7	1.8	5.5
26	92.8	1.7	5.5
27	92.3	1.7	6.0
28	92.7	1.7	5.6
29	49.1	3.1	47.8
30	48.7	3.0	48.3
31	92.9	1.8	5.3
32	92.6	1.9	5.5
33	92.2	1.8	6.0
34	92.2	1.8	6.0
35	52.4	3.0	44.6
36	51.0	3.2	45.8

Table III. EDS Analysis of Marked Points in Fig. 4 of Soldering Joints with Increasing Temperatures of 450 °C, 475 °C, and 500 °C and a Time of 3 Min

	Weight Percent		
	MgK	AlK	ZnK
37	96.0	0.2	3.8
38	95.2	0.2	4.6
39	49.3	0.9	49.8
40	49.9	0.9	49.2
41	94.4	0.3	5.3
42	95.5	0.6	3.9
43	95.6	0.6	3.8
44	95.7	0.5	3.8
45	57.2	1.6	41.2
46	56.0	1.6	42.4
47	96.5	0.5	3.0
48	95.5	0.6	3.9
49	96.5	0.5	3.0
50	96.4	0.5	3.1
51	96.5	0.4	3.1
52	55.4	1.7	42.9

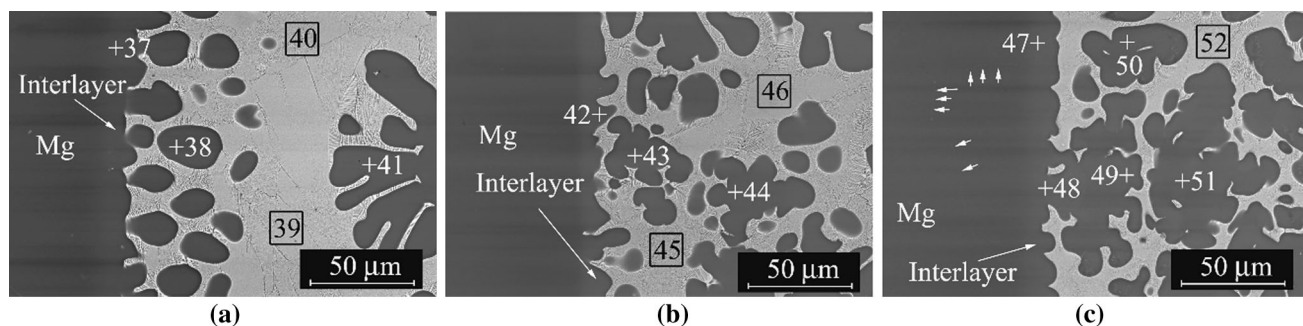


Fig. 3—Microstructure of eutectic Zn-Al with Mg joints after soldering for 3 min at temperatures of (a) 450, (b) 475, and (c) 500 °C. The numbers in the figure denote the points of EDSs presented in Table III.

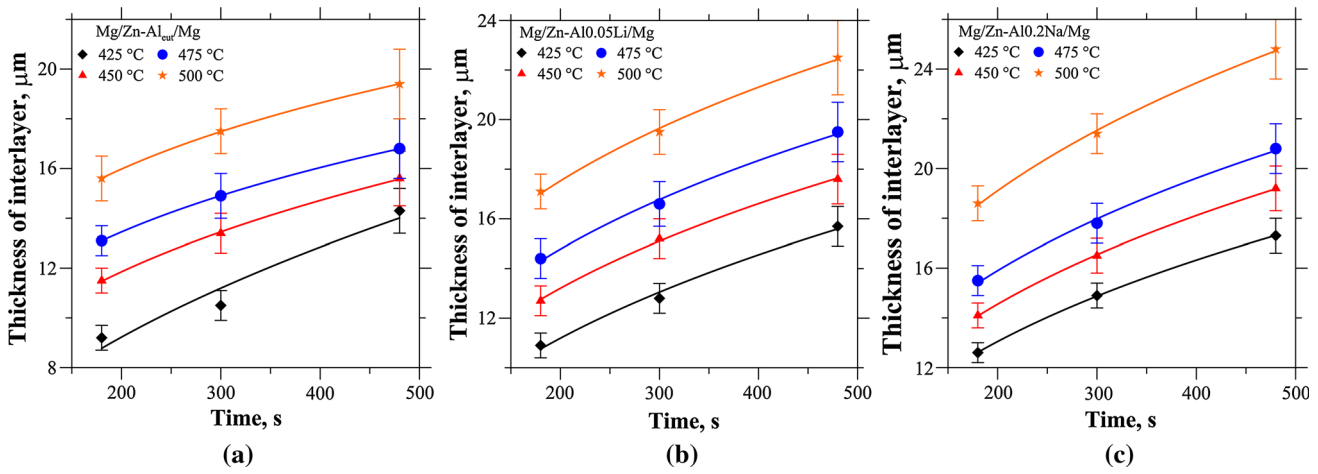


Fig. 4—Thickness of the interlayer at the interface after soldering process for (a) Zn-Al, (b) Zn-Al0.05Li, (c) Zn-Al0.2Na, respectively, as a function of time for different temperatures.

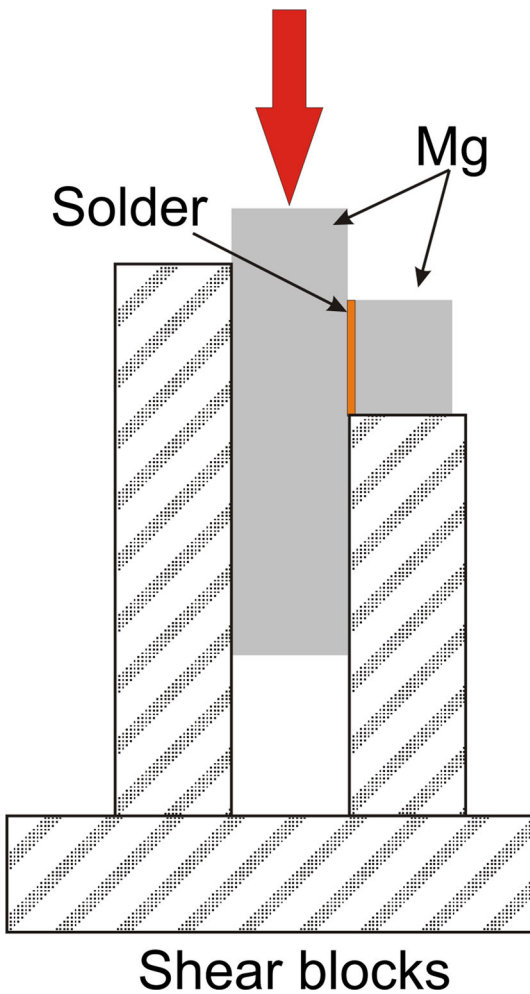


Fig. 5—Device and samples for shear strength measurements.

interface reaction area, which results in the Mg substrate being dissolved by solders at the high temperature of 500 °C.

Table IV shows the microhardness of eutectic Zn-Al and Zn-Al alloys with Li and Na on Mg substrate. The two regions investigated were the α -Mg + MgZn eutectoid structure and the α -Mg solid solution. The average microhardnesses obtained for the α -Mg region were 103, 104, and 101 ($HV_{0.05}$) for eutectic Zn-Al, and Zn-Al with Li and Na, respectively. The microhardness of the α -Mg region was related to the amount of doped Zn and Al, which was shown in the EDS analysis collected in Tables I through III. The average microhardnesses obtained for the α -Mg + MgZn region were 243, 233, and 237 ($HV_{0.05}$) for eutectic Zn-Al, and Zn-Al with Li and Na, respectively. The same situation as for the α -Mg region occurs, so the addition of Li and Na increase microhardness to 67.2^[13] and 56.6^[14] ($HV_{0.05}$), respectively, compared to eutectic Zn-Al (55.0 ($HV_{0.05}$)^[13]). However, the greater addition of Na to eutectic Zn-Al caused the creation of an area of doped NaZn₁₃, where the microhardness is much higher (for Na (3 wt pct) it is 339.0 ($HV_{0.05}$)^[13]). In the case of soldering AZ31 using the Zn-Al filler metal,^[19] the average microhardness values obtained at the interface of the α -Mg solid solution and α -Mg + MgZn eutectoid structure are 93 and 134 ($HV_{0.05}$), respectively, compared to 81 ($HV_{0.05}$) and 130 ($HV_{0.05}$), respectively, for Zn-Mg-Al solder, which is much lower than for the α -Mg + MgZn region result obtained by this study.

IV. DISCUSSION

During the soldering process, Zn-Al solders and the Mg substrate formed an interfacial layer at the interface. This is a diffusion layer, where the α -Mg solid solution is contained by Zn and Al. Such behavior was observed for solder materials of the Zn-Al system,^[18] Zn-Mg-Al,^[23] Zn-Mg,^[9] and Sn-Zn.^[10] The Mg substrate dissolves more easily compared to a Cu substrate,^[15–18] and the kinetics of creation of the IMC layer are different. However, the interlayer after soldering for 8 minutes at a temperature of 500 °C is not as thick as

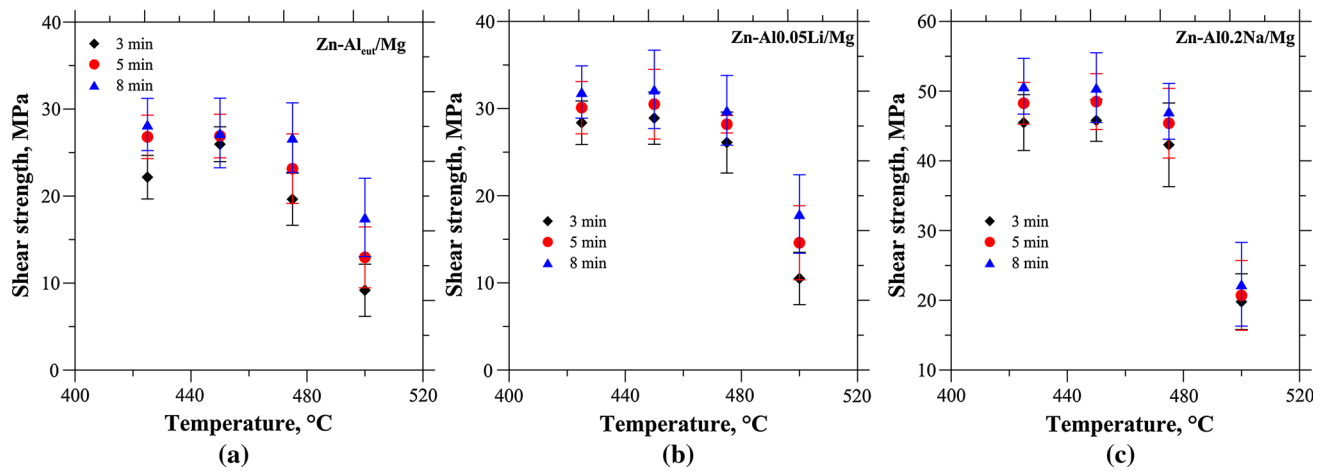


Fig. 6—Shear strength of joints for (a) eutectic Zn-Al, (b) Zn-Al0.05Li, and (c) Zn-Al0.2Na, respectively.

Table IV. Microhardness Value Obtained at the Interface of Mg Joints for Eutectic Zn-Al, Zn-Al0.05Li, and Zn-Al0.2Na Alloys

Alloys	Microhardness (HV)	
	α -Mg Region	α - Mg + MgZn Region
Zn-Al.	103 \pm 4	243 \pm 7
Zn-Al0.05Li	104 \pm 4	233 \pm 2
Zn-Al0.2Na	101 \pm 3	237 \pm 11

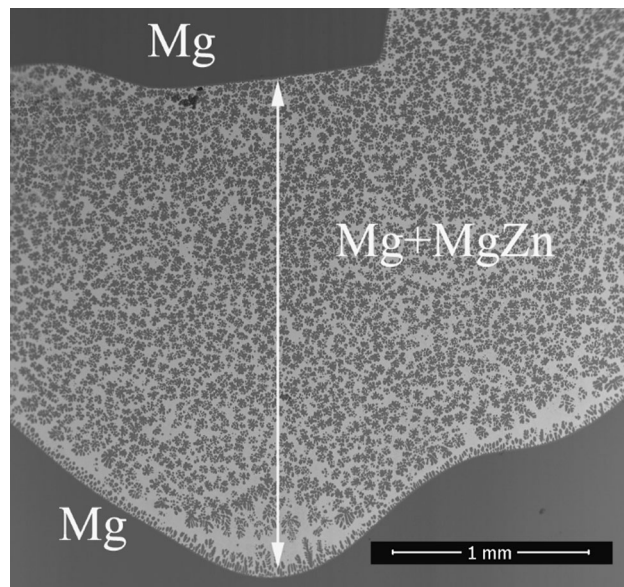


Fig. 7—Microstructures of eutectic Zn-Al with Mg substrates joints after soldering at a temperature of 475 °C for 8 min.

that of the same solder used for soldering Cu (87.1 μ m for Zn-Al,^[24] 85.5 μ m for Zn-Al0.05Li,^[15] and 79.3 μ m for Zn-Al0.2Na,^[16] compared to this study: 19.4, 22.5, and 24.8 μ m, respectively). In the case of the Cu substrate, three IMCs ϵ -CuZn₄, γ -Cu₅Zn₈, and

β -CuZn are formed at the interface during soldering, causing the pure Cu to dissolve in the solder but only as particles of ϵ , which could with time transform to the γ phase as the phase with lower Gibbs free energy.^[16,25,26] The observed microstructure of Mg joints (Figures 1, 2 and 3) shows that the Mg from the substrate dissolved in the solder as particles of Mg (EDS points: 6, 9, 10, 17, 19, and so on), and as the matrix of solder α - Mg + MgZn (area EDS: 4, 5, 11, 12, 16, 18, and so on). The solder's chemical composition transforms from the Zn-Al system to the Mg-Zn system in the event of diffusion of Mg from the substrate. A different character of changes is observed for Cu joints,^[18] where the Cu dissolves in the solder but the matrix of the solder is still the Zn-Al system. For such changes, temperature controls the reaction when soldering on Mg substrate. For the Mg-Zn system,^[19] the temperature of the soldering process is above that of eutectic reaction, so the Mg will dissolve faster in the solder. As observed in References 2, 23, and 24 and in our study, the Mg substrate is dissolved in the solder in its entirety, and the amount of Mg increased with increasing soldering time. The results show that the relative content of Al and Zn elements in the solder decreases. The Mg substrate dissolves in a similar manner as in the dissolving ϵ phase in the solder, with “scallops” detaching from the interlayer and diffusing deeper in the solder. The amount of Mg in the solder matrix close to the interlayer was similar to the amount in Reference 10 in which the composition of the solder was 47.8 of Mg, 48.9 of Zn and 3.3 of Al (wt pct), as it was in this study (EDS analysis, Tables I through III). However, as presented in Reference 10, for soldering at 390 °C for 30 seconds, with solder composed of 97.7 Zn, 0.8 Mg, 1.1 Al and 0.4 Mn (wt pct), the Zn reach region is observed within the solder.^[10] This changes with a higher amount of Mg in the solder (83.0 of Zn, 15.2 of Mg, 1.3 of Al, and 0.5 Mn (wt pct)), and the Zn reach region almost disappears at a slightly higher soldering temperature (420 °C). In this study, after 3 minutes and at a soldering temperature of 475 °C, the chemical composition of solder was Mg + MgZn, as shown in Figure 7.

As observed in Reference 10, the weld width (joint area) is increased from 378 to 722 μm , indicating that the diffusion of Mg is higher than that of Zn and Al. However, the process of dissolution of the Mg substrate is very dynamic, as it happens spontaneously rather than uniformly, creating a place where there is a fast path of Mg diffusion to the solder (as shown in Figure 7). The model of microstructure evaluation of Mg/Zn/Mg joints was presented in Reference 27. At first, in the case of dissolving Mg substrate by Zn, an interlayer starts to be created at the interface. The “scalped” structure of the interlayer is correlated with the grain boundary penetration phenomenon: liquid would penetrate the grain boundary along the depth direction of the Mg-base metal, since the Mg atoms at the grain boundary had higher chemical potential than those in the grains.^[28] At higher temperatures, the diffusion coefficient of Mg increased exponentially, causing an increase in the Mg contained in the liquid and increasing the width of the Mg(Zn) diffusion layer.^[27] The same character of dissolving substrate and formation of “scalps” at the interface as that presented in the literature for Cu substrate with Zn-Al alloys was observed.^[15–18] However, in the case of Cu, three IMCs were formed at the interface and the process was controlled by the diffusion of Cu to the solder (Table IV).

Taking into account that the thickness of the IMC layer is correlated with diffusion and growth rate in the Mg joint, the character of growth rate changes from volume diffusion to grain boundary. However, a lot of Mg particles are observed in the solder. Similar microstructure and properties for Mg joints soldered with Zn-based alloys were observed in the literature^[9,19,23] for Al-based filler metal.^[24] The diffusion layer at the interface is observed, and a huge amount of Mg dissolves in solder and changes its chemical composition to $\alpha\text{-Mg} + \beta\text{-Mg}_{17}\text{Al}_{12}$. The results of the performed mechanical tests indicate that the average shear strength is 45 MPa.^[24] Furthermore, the fractographic analysis of the soldered Mg joint for both Zn and Al-based solder shows a brittle fracture pattern.^[9,18,23,24]

The results of mechanical property testing showed that the addition of Li and Na increases the shear strength of Mg joints to ~ 32 and ~ 50 MPa, respectively, compared to 28 MPa for eutectic Zn-Al. Furthermore, the obtained shear strength is slightly higher compared to 19 MPa^[19] for a Zn-Al alloy filler with 19.2 (wt pct) Al. However, this is much lower compared to 70 MPa for Sn40Zn^[10] and 56 MPa for Mg3.0Al1.0Zn0.4Mn0.1Si.^[23] Moreover, as was observed in all cases, the fracture proceeds from the eutectic $\alpha - \text{Mg} + \text{MgZn}$ region close to the interfacial layer. The observation in Reference 19 shows that the fracture of the soldered joint has a brittle pattern. The dissolution of Al and Zn in the $\alpha\text{-Mg}$ has a solid solution strengthening effect, which improved the mechanical properties. The stress concentration effect in solder joints on Mg substrate accumulates in the $\alpha - \text{Mg} + \text{MgZn}$ eutectoid structure, where the fracture will start. The authors^[19] show that the high microhardness and brittleness of the $\alpha - \text{Mg} + \text{MgZn}$ eutectoid structure in the case of Zn-Al solder are the main reasons for the fracture of the soldered Mg joints. The fracture-causing high microhardness of the $\alpha - \text{Mg} + \text{MgZn}$ eutectoid structure is 134 (HV_{0.05}),

compared to 93 (HV_{0.05})^[19] for the $\alpha\text{-Mg}$ solid solution. As presented in Reference 23 for Mg-based solder, the fracture of the joint exhibits intergranular features, and the crack originates from the $\alpha - \text{Mg} + \text{MgZn}$ eutectoid structure. The microhardness of the $\alpha\text{-Mg}$ solid solution is 81 (HV_{0.05}), and that of the $\alpha - \text{Mg} + \text{MgZn}$ eutectoid structure is 130 (HV_{0.05}).^[23] Where an external force acts on the solder joint, the stress concentration is generated easily from the hard $\alpha - \text{Mg} + \text{MgZn}$ eutectoid structure.^[23] The same effect as in the case of Zn-Al^[19] and Mg-based^[23] solders was observed for Al-based solder,^[24] where the hard phase of $\beta\text{-Mg}_{17}\text{Al}_{12}$ (which is much harder than $\alpha\text{-Mg}$, at 120 (HV_{0.05}) and 91 (HV_{0.05}), respectively) is responsible for the fracture. The same observation is made in Reference 8—that, with increasing Al in Mg-Sn-In-Al, the hardness also increases, from 96 (HV_{0.05}) to 123 (HV_{0.05}) for 0 and 6 (wt pct) of Al, respectively. For the higher microhardness values for $\alpha\text{-Mg}$ (~ 100 (HV_{0.05})) and $\alpha\text{-Mg} + \text{MgZn}$ (~ 230 (HV_{0.05})) obtained in this study, the fact that the soldering process was performed without flux had an impact. This could be compared with References 19 and 23, where soldering was carried out in the presence of QJ201 flux—which in our observations and measurements reduced the mechanical properties of the obtained joints.

V. CONCLUSIONS

Eutectic Zn-Al, Zn-Al0.05Li, and Zn-Al0.2Na alloys were designed to join pure magnesium substrate. The experiment shows the mechanism and morphology changes for Mg, forming the basis of and explain the behavior of Mg when soldering Mg alloys. From this study, the following important conclusions were derived:

- (1) Magnesium substrate can be successfully joined by eutectic Zn-Al, Zn-Al0.05Li, and Zn-Al0.2Na alloys in an argon gas shield.
- (2) The original solder, eutectic Zn-Al, Zn-Al0.05Li, and Zn-Al0.2Na alloys were consumed after the soldering process. The cross section microstructure showed that $\alpha - \text{Mg} + \text{MgZn}$ eutectoid structures were formed in the soldering region.
- (3) The average shear strengths are 28, 32, and 50 MPa for eutectic Zn-Al, Zn-Al0.05Li, and Zn-Al0.2Na alloys, respectively, for soldered Mg joints. The microhardness for the $\alpha\text{-Mg}$ region is 103, 104, and 101 (HV_{0.05}), and for $\alpha - \text{Mg} + \text{MgZn}$ is 243, 233, and 237 (HV_{0.05}) for eutectic Zn-Al, Zn-Al0.05Li, and Zn-Al0.2Na, respectively. The fracture is intergranular, and the crack originates from the hard $\alpha - \text{Mg} + \text{MgZn}$ eutectoid structure.

OPEN ACCESS

This article is distributed under the terms of the Creative Commons Attribution 4.0 International License (<http://creativecommons.org/licenses/by/4.0/>), which permits unrestricted use, distribution, and reproduction in any medium, provided you give appropriate credit to the original author(s) and the source, provide a link to the Creative Commons license, and indicate if changes were made.

REFERENCES

1. K.U. Kainer, ed., *Magnesium Alloys and their Applications*, ed., Wiley-Vch, New York, 2006.
2. A.A. Luo: *Inter. Mater. Rev.*, 2004, vol. 49, pp. 13–30.
3. Y. Zhang, Z. Luo, Y. Li, Z.-M. Liu, and Z.-Y. Huang: *Mat. Des.*, 2015, vol. 75, pp. 166–73.
4. J. Hirsch and T. Al-Samman: *Acta Mater.*, 2013, vol. 61, pp. 818–43.
5. M. Mezbahul-Islam, A.O. Mostafa, and M. Medraj: *J. Mater.*, 2014, vol. 2014, pp. 1–33.
6. F. Hayat: *Mater. Des.*, 2011, vol. 32, pp. 2476–84.
7. L.M. Zhao and Z.D. Zhang: *Scr. Mater.*, 2008, vol. 58, pp. 283–86.
8. L.M. Liu and H.Y. Wang: *Mater. Sci. Eng. A*, 2009, vol. 507, pp. 22–28.
9. L. Liu and Z. Wu: *Mater. Character.*, 2010, vol. 61, pp. 13–18.
10. Z. Wang, H. Wang, and L. Liu: *Mat. Des.*, 2012, vol. 39, pp. 14–19.
11. T. Watanabe, 8 – Brazing and soldering of magnesium alloys, Welding and joining of magnesium alloys, (2010) 97-121.
12. M.K. Kulekci: *Int. J. Adv. Manuf. Technol.*, 2008, vol. 39, pp. 851–65.
13. T. Gancarz, G. Cempura, and W. Skuza: *Mater. Charact.*, 2016, vol. 111, pp. 147–53.
14. T. Gancarz and G. Cempura: *Mater. Des.*, 2016, vol. 104, pp. 51–59.
15. T. Gancarz, J. Pstrus, G. Cempura, and K. Berent: *J. Electron. Mater.*, 2016, vol. 45, pp. 6067–78, <https://doi.org/10.1007/s11664-016-4815-8>.
16. T. Gancarz and J. Pstrus: K. Berent: *J. Mater. Eng. Perform.*, 2016, vol. 25, pp. 3366–74, <https://doi.org/10.1007/s11665-016-2075-7>.
17. J. Pstrus, P. Fima, and T. Gancarz: *J. Mater. Eng. Perform.*, 2012, vol. 21, pp. 606–13.
18. J. Pstrus and T. Gancarz: *J. Mater. Eng. Perform.*, 2014, vol. 23, pp. 1614–24.
19. L. Ma, D.Y. He, X.Y. Li, and J.M. Jiang: *Mater. Letter.*, 2010, vol. 64, pp. 596–98.
20. T. Massalski, H. Okamoto, P. Subramanian, and L. Kacprzak: *Binary alloy phase diagrams*, ASM International, Ohio, 2001, p. 2445.
21. J.R. Terbush, N. Stanford, J.-F. Nie, and M.R. Barnett: *Metall. Mater. Trans. A*, 2013, vol. 44A, pp. 5216–24.
22. M. Prazmowski: *Arch. Metall. Mater.*, 2014, vol. 59, pp. 1137–42.
23. L. Ma, D. He, X. Li, and J. Jiang: *J. Mater. Sci. Technol.*, 2010, vol. 26, pp. 743–46.
24. L. Ma, P. Qiaoa, W. Longa, D. Heb, and X. Lib: *Mater. Des.*, 2012, vol. 37, pp. 465–69.
25. T. Gancarz, J. Pstrus, P. Fima, and S. Mosinska: *J. Alloy Compd.*, 2014, vol. 582, pp. 313–22.
26. Y. Takaku, L. Felicia, I. Ohnuma, R. Kainuma, and K. Ishida: *J. Electron. Mater.*, 2008, vol. 37, pp. 314–23.
27. R. Xie, X. Chen, Z. Lai, L. Liu, G. Zou, J. Yan, and W. Wang: *Mater. Des.*, 2016, vol. 91, pp. 19–27.
28. M.F. Wu, C. Yu, and J. Pu: *Mater. Sci. Technol.*, 2008, vol. 24, pp. 1422–26.